catalysts

MDPI

Article

Photoassisted Oxidation of Sulfides Catalyzed by Artificial Metalloenzymes Using Water as an Oxygen Source †

Christian Herrero [1], Nhung Nguyen-Thi [2], Fabien Hammerer [1], Frédéric Banse [1], Donald Gagné [2], Nicolas Doucet [2], Jean-Pierre Mahy [1,*] and Rémy Ricoux [1,*]

[1] Institut de Chimie Moléculaire et des Matériaux d'Orsay UMR 8182 CNRS, Bâtiment 420, Université Paris Sud, Université Paris Saclay, F-91405 Orsay CEDEX, France; christian.herrero@u-psud.fr (C.H.); fabien.hammerer@gmail.com (F.H.); frederic.banse@u-psud.fr (F.B.)

[2] Institut National de la Recherche Scientifique (INRS)-Institut Armand-Frappier, Université du Québec, 531 Boulevard des Prairies, Laval, QC H7V 1B7, Canada; tepnhung@yahoo.com (N.N.-T.); donald.gagne@asrc.cuny.edu (D.G.); nicolas.doucet@iaf.inrs.ca (N.D.)

* Correspondence: jean-pierre.mahy@u-psud.fr (J.-P.M.); remy.ricoux@u-psud.fr (R.R.); Tel.: +33-1-69-15-74-21 (J.-P.M.); +33-1-69-15-47-23 (R.R.)

† Dedicated to the memory of Dr. Dominique Mandon.

Academic Editors: Jose M. Palomo and Cesar Mateo
Received: 19 October 2016; Accepted: 6 December 2016; Published: 12 December 2016

Abstract: The Mn(TpCPP)-Xln10A artificial metalloenzyme, obtained by non-covalent insertion of Mn(III)-meso-tetrakis(*p*-carboxyphenyl)porphyrin [Mn(TpCPP), **1**-Mn] into xylanase 10A from *Streptomyces lividans* (Xln10A) as a host protein, was found able to catalyze the selective photo-induced oxidation of organic substrates in the presence of $[Ru^{II}(bpy)_3]^{2+}$ as a photosensitizer and $[Co^{III}(NH_3)_5Cl]^{2+}$ as a sacrificial electron acceptor, using water as oxygen atom source.

Keywords: artificial metalloenzyme; manganese porphyrin; light induced oxidation

1. Introduction

Over the past few decades, the need for economically and environmentally compatible chemical processes has increased exponentially, along with global environmental concerns. As a result, the concept of green chemistry has emerged, which endorses the use of mild chemical reaction conditions, such as the use of non-polluting reactants, visible light as main energy source, and water as solvent, which, in addition, serves as O atom and electron sources [1]. In this context, oxidation reactions such as the conversion of alkanes into alcohols—one of first steps in the synthesis of products issued from the petrochemical industry—would benefit from significant improvements. Current chemical processes take place in wasteful organic solvents at high temperature, in addition to lacking in efficiency and/or selectivity [2,3]. Although promising metal catalysts have been developed and show encouraging implementation potential [4], several aspects such as efficacy, regio- and stereoselectivity, compound stability, or environmental toxicity remain to be addressed. In addition, these reactions often resort to oxidant reactants that might have a direct or indirect impact on the environment [2,3].

Natural enzymes provide us with astonishing examples of extremely efficient, selective, and stable catalysts. Oxidases constitute a widely investigated class of enzymes, most of which contain one or several metal ions at the heart of their redox center. For example, a non-heme iron enzyme such as phenylalanine hydroxylase (PAH) [5] catalyzes the hydroxylation of the aromatic side-chain of phenylalanine to generate tyrosine, whereas di-iron enzymes such as methane monooxygenases (MMO) allow the transformation of methane into methanol [6,7]. Cytochrome P450 enzymes constitute a large family of hemoproteins that can perform the oxidation of various substrates at high catalytic rates

using molecular oxygen as the sole source of oxidant through a reductive activation mechanism [8]. During the catalytic cycle, two electrons are provided by redox mediators, Nicotinamide Adenine Dinucleotide (NADH), Nicotinamide Adenine Dinucleotide phosphate (NADPH), etc., allowing the formation of a very reactive high-valent iron-oxo intermediate responsible for substrate oxidation.

Over the years, P450 enzymes have been largely studied and utilized for catalytic purposes. However, electron delivery to the iron center remains the principal hurdle to high catalytic efficiency. On the one hand, natural redox cofactors are expensive, requiring the need to recycle them or to avoid their use. On the other hand, the electrons are not directly transferred to the heme iron, but instead are delivered through a P450 reductase that involves two flavin redox cofactors, i.e., Flavin Adenine Dinucleotide (FAD) and Flavin Mononucleotide (FMN). Two electrons are initially transferred from NADPH to FAD to yield $FADH_2$, which then transfers them to FMN. The obtained $FMNH_2$, then delivers sequentially, one by one, these two electrons to the iron atom at precise steps of the catalytic cycle [9]. Such a complex process, which is also driven by protein conformational changes, is then far from reproducible, and numerous approaches have been developed to mimic this catalytic reaction. For instance, approaches like the use of alternative oxygen atom donors (PhIO, ROOH, H_2O_2, $KHSO_5$, etc.) [10], chemical or electrochemical reductions [11], and, more recently, reductase proteins that were substituted with ruthenium-based photosensitizers capable of gathering electrons upon light irradiation and transferring them to cytochrome (P450) enzymes [12,13].

This latter field of research is appealing because it utilizes visible light as the sole energy input in the chemical reaction, which can be used either under reductive or oxidative experimental conditions. The former pathway relies on the photo-reduction by diethyldithiocarbamate (DTC) of a Ru^{II}-chromophore that is covalently attached to the apo-P450, which then catalyzes the reductive activation of oxygen leading, in the presence of H^+, to a high-valent P450Fe^{V}-oxo species that performs the oxidation of fatty acids [12,13]. Conversely, the oxidative pathway relies on the ability to quench the excited state of a $[Ru^{II}(bpy)_3]^{2+}$ chromophore with an irreversible electron acceptor such as $[Co^{III}(NH_3)_5Cl]^{2+}$, in order to form the highly oxidative $[Ru^{III}(bpy)_3]^{3+}$, which then catalyzes the two-electron oxidation of an iron-bound water molecule with formation of the high-valent iron-oxo species (Scheme 1, Path a) [14].

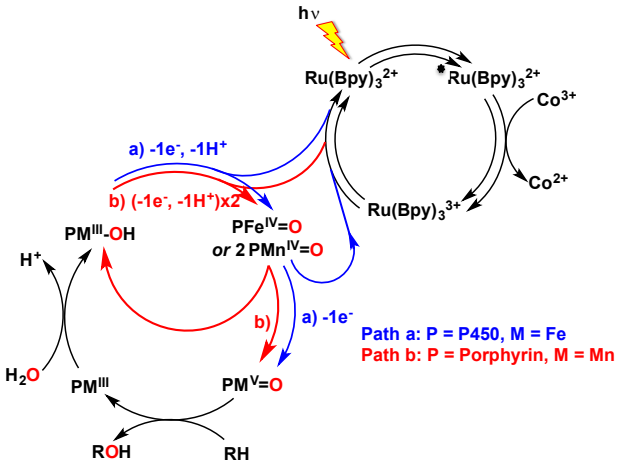

Scheme 1. Reaction pathways for the two-electron oxidation of an organic substrate by light-driven activation of a catalyst: Path (**a**) two-electron oxidation of an iron-bound water molecule into high-valent P-450-iron-oxo species by $[Ru^{III}(bpy)_3]^{3+}$, generated by quenching of the excited state of $[Ru^{II}(bpy)_3]^{2+}$ by an irreversible electron acceptor ($[Co^{III}(NH_3)_5Cl]^{2+}$) [14]; Path (**b**) one-electron oxidation of an Mn^{III}-OH complex into a porphyrin-Mn^{IV}-oxo species by $[Ru^{III}(bpy)_3]^{3+}$, followed by the disproportionation of the Mn^{IV}-oxo species into Mn^{III} and Mn^{V}=O [15,16].

The oxidative pathway was also used with biomimetic systems involving manganese porphyrins as catalysts and water as an oxygen source, which were reported originally by Calvin's group [15], and more recently by Fukuzumi et al. [16]. In these systems, the authors showed that the photogenerated highly oxidative $[Ru^{III}(bpy)_3]^{3+}$ can oxidize the Mn^{III}-OH complex into an Mn^{IV}-oxo species. In this case, the Mn^{V}-oxo species was not directly formed by a second one-electron oxidation, but rather arose from the disproportionation of the Mn^{IV}-oxo species into Mn^{III} and Mn^{V}=O (Scheme 1, Path b) [16]. Such a system could catalyze the oxidation of water-soluble substrates, including alkenes, alkanes, and sulfides [16]. Previous work from our group also showed that the moderately enantioselective light-induced oxidation of thioanisole by water as the oxygen atom source could occur in the presence of a system that associated a protein that induced chirality, BSA (Bovine Serum Albumin), a manganese corrole as oxygen atom transfer catalyst, and $[Ru^{II}(bpy)_3]^{2+}$ as photosensitisizer [17].

In parallel, other work also allowed us to show the strong affinity of manganese sodium tetra-*para*-carboxylatophenyl-porphyrin (Mn-TCPP) for xylanase 10A (Xln10A) from *Streptomyces lividans*, a glycoside hydrolase that catalyzes the hydrolysis of (1-4)-β-D-xylosidic bonds in xylan biopolymers to release xylose [18]. Xylanase 10A is an abundant and resistant protein. It is easily purified and its sequence and three-dimensional structure are known, which makes it a good candidate as a protein scaffold for the production of biohybrid catalysts resulting from the combination of a natural protein and an artificial metal complex. We expected this combination of enzymatic and molecular catalysis to yield hybrid catalysts showing improved efficacy, selectivity, and stability. Studies on the reactivity of the Mn-TCPP-Xln10A hybrid showed that it possessed good mono-oxygenase activity for the epoxidation of styrene-type compounds, in addition to yielding important enantiomeric excesses, in particular for the epoxidation of *p*-methoxystyrene by oxone. This selectivity was further illustrated by molecular modeling studies that showed the existence of hydrogen bonds between the methoxy substituent of the substrate and a tyrosine residue of the protein [18].

We thus decided to use our Mn-TCPP-Xln10A biohybrid as a catalyst for the selective photo-induced oxidation of organic substrates in the presence of $[Ru^{II}(bpy)_3]^{2+}$ as a photosensitizer and $[Co^{III}(NH_3)_5Cl]^{2+}$ as a sacrificial oxidant, with water as an oxygen atom source. We report that both Mn-TCPP and its complex with xylanase 10A can catalyze the photoinduced sulfoxidation of thioanisole and 4-methoxythioanisole with slight enantiomeric excesses, using water as an oxygen atom source.

2. Results

2.1. Preparation of the Catalysts

Meso-tetrakis-*para*-carboxyphenylporphyrin **1** was first prepared in a 10.5% yield by condensation of p-carboxybenzaldehyde with pyrrole in propionic acid according to the procedure of Adler et al. [19,20]. Its Electon Spray Ionisation Mass (ESI-MS) and Ultra-Violet-visible (UV-vis) spectroscopy characteristics were found identical to those already reported [19]. The insertion of manganese was performed by treatment of **1** with an excess of $Mn(OAc)_2$, 4 H_2O in 50 mM AcONa buffer, and pH 4.0 at 100 °C for 4 h, as described in the experimental section. The excess manganese salt was then removed by two successive purifications, first on P6DG exclusion gel, and second on Chelex. After lyophylization, **1**-Mn was obtained in a quantitative yield and characterized by ESI-MS and UV-vis spectroscopy, in agreement with those already reported [18] and with an Mn(T*p*CPP) structure (Figure 1).

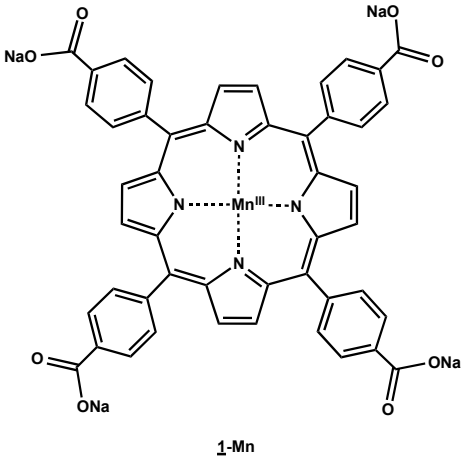

Figure 1. Manganese(III)-meso-tetrakis-*para*-carboxyphenylporphyrin, **1**-Mn.

To prepare the **1-**Mn-Xln10A artificial hemoprotein, xylanase 10A (Xln10A) was first purified from the supernatant of *S. lividans* culture as reported earlier [21]. Solutions of the artificial hemoprotein were then prepared by incubating Xln10A in 50 mM sodium phosphate buffer, pH 7.0 with various amounts of **1-**Mn for 30 min. at room temperature. **1-**Mn-Xln10A was then characterized by UV-visible spectroscopy as described above, and its UV-visible spectrum was similar to that of **1-**Mn alone, with maxima at 468, 566 and 599 nm in 50 mM sodium phosphate buffer pH 7.0.

UV-visible spectroscopy could thus not be used for the determination of the stoichiometry and of the dissociation constant of the **1-**Mn-Xln10A. Since, in addition, **1-**Mn-Xln10A dissociates under mass spectrometry analysis conditions, the binding affinity of the **1**-Mn complex for Xln10A was then studied by measuring the quenching of the fluorescence of the tryptophan residues of Xln10A, 5 μM in 50 mM sodium phosphate buffer pH 7.0 at 25 °C as a function of the **1**-Mn concentration as previously reported [18]. The quenching was complete and selective, and suitable data were obtained from plots of fluorescence intensity versus the Xln10A/**1**-Mn ratio. A double reciprocal plot of the residual fluorescence intensity at 340 nm as a function of the **1**-Mn final concentration allowed calculation of a K_D value of 1.5 μM for **1**-Mn-Xln10A and determined that only one ligand was bound per protein [18]. This K_D value was similar to that already reported for the Fe(T*p*CPP)-Xln10A complex (K_D = 0.5 μM) [21], and was in agreement with the fact that the binding of the porphyrin cofactor occurred thanks to interactions of three of its carboxylate substituents with amino-acid side chains of the protein and that no amino-acid side chain was interacting with the metal cation. This could be explained after molecular modeling calculations [18].

Taking into account the K_D values measured for **1**-Mn-Xln10A, it was possible to calculate the theoretical concentration of protein necessary to bind 100% of the metal cofactor. It was thus found that four equivalents of Xln10A were necessary to bind one equivalent of the **1**-Mn cofactor. Accordingly, when the effect of the Xln10A/**1**-Mn ratio on the oxidation of styrene derivatives by $KHSO_5$ catalyzed by **1**-Mn-Xln10A in 50 mM phosphate buffer, pH 7.0, it appeared that the total yield of the reaction as well as its chemoselectivity and the enantiomeric excesses observed for the obtained epoxides were optimal when four equivalents of Xln10A were used with respect to **1**-Mn. It was thus decided to perform the photoassisted oxidation of sulfides in the presence of Xln10A and **1**-Mn in a 4/1 ratio as catalyst.

2.2. Catalysis

The oxidation of thioanisole (3200 eq.) 99 mM in 50 mM phosphate buffer solution (pH 7.0) was first assayed in the presence of 0.42 mM $[Ru^{II}(bpy)_3]^{2+}$ (13 eq.) as a photosensitizing agent, 12 mM $[Co^{III}(NH_3)_5Cl]^{2+}$ (390 eq.) as an irreversible electron acceptor and 32.5 μM **1**-Mn (1 eq.) in the presence of 130 μM Xln10A (4.2 eq.) (Xln10A/1-Mn ratio = 4) as catalyst (Scheme 2).

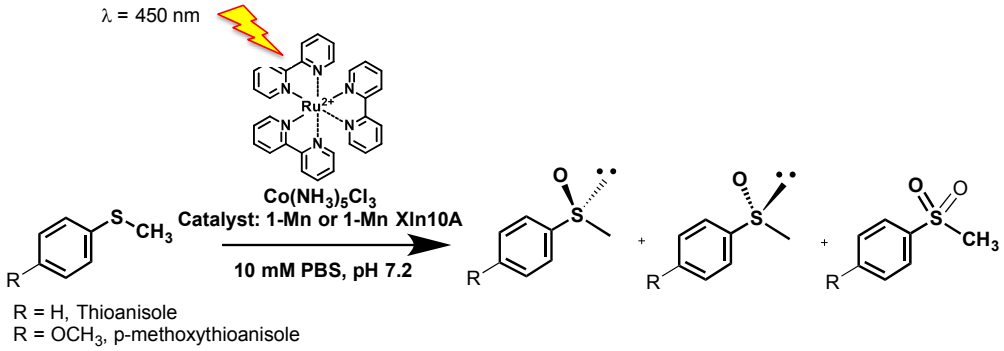

Scheme 2. Photoassisted oxidation of thioanisole and *p*-methoxythioanisole in the presence of $[Ru^{II}(bpy)_3]^{2+}$ as a photosensitizing agent, $[Co^{III}(NH_3)_5Cl]^{2+}$ as an irreversible electron acceptor and **1**-Mn or **1**-Mn-Xln10A as a catalyst.

When control experiments were run either in the absence of catalyst or in the absence of the $[Ru^{II}(bpy)_3]^{2+}$ photosensitizing agent, no oxidation products were formed. On the contrary, when the reaction was run in the presence of $[Ru^{II}(bpy)_3]^{2+}$ and of either **1**-Mn or **1**-Mn-Xln10A as catalyst, methylphenylsulfoxide was obtained as the major product. A Turnover number (TON) of 125 ± 5 was obtained after the photo driven reaction of **1**-Mn with $[Ru^{II}(bpy)_3]^{2+}$ in the absence of protein, which corresponds to a 64% yield with respect to $[Co^{III}(NH_3)_5Cl]^{2+}$. Minor amounts of sulfone (6 ± 1 TON) were also formed (Table 1). Further HPLC analysis showed that a racemic mixture of methylphenylsulfoxide was produced, and thus that the reaction was not enantioselective. When the experiment was performed in the presence of Xln10A, methylphenylsulfoxide was obtained as the sole product with a TON of 25 ± 2 (13% yield with respect to $[Co^{III}(NH_3)_5Cl]^{2+}$). After HPLC analysis, no enantiomeric excess could be measured, showing that under those conditions the protein did not induce any stereoselectivity.

Table 1. Products obtained upon photoassisted oxidation of thioanisole in the presence of $[Ru^{II}(bpy)_3]^{2+}$ as a photosensitizing agent, $[Co^{III}(NH_3)_5Cl]^{2+}$ as electron acceptor, and various catalysts including **1**-Mn-Xln10A and **1**-Mn.

Substrate	Catalyst	Products (TON) Sulfone	Products (TON) Sulfoxide	Enantiomeric Excess (ee) (%)	Reference
Thioanisole (*R* = H)	**1**-Mn [a]	6 ± 1	125 ± 5	0	This work
	1-Mn-Xln10A [a]	-	25 ± 2	0	This work
	Mn-Corrole	1.6	32 ± 3	0	[17]
	Mn-Corrole-BSA	-	21 ± 7	12–16	[17]
	Ru_{Phot}-Ru_{Cat}-H_2O [b]	-	745	-	[22]
p-Methoxy-thioanisole (*R* = OCH_3)	**1**-Mn [a]	-	100 ± 4	0	This work
	1-Mn-Xln10A [a]	-	10 ± 1	7 ± 1	This work
	Ru_{Phot}-Ru_{Cat}-H_2O [b]	-	709	-	[22]
p-Bromo-thioanisole (*R* = Br)	Ru_{Phot}-Ru_{Cat}-H_2O [b]	-	314	-	[22]
	Ru_{Phot}-Ru_{Cat}-H_2O [c]	-	201	-	[23]
2-(CH_3-thio)ethanol	Mn-TMPS [c]		30		[16]

[a] Conditions as described in the experimental section; $[Ru^{II}(bpy)_3]^{2+}$ = ruthenium-tris-bipyrridyle, $[Co^{III}(NH_3)_5Cl]^{2+}$ = Cobalt-pentammine chloride, Xln 10A = xylanase 10A, Manganese(III)-meso-tetrakis-*para*-carboxyphenylporphyrin = **1**-Mn [b] Ru_{Phot}-Ru_{Cat}-H_2O = ($[(bpy)_2Ru(4\text{-}Me\text{-}BPy\text{-}terPy)Ru(bpy)\text{-}(OH_2)]^{4+}$; [b] Ru_{Phot}-Ru_{Cat}-H_2O = ($[(bpy)_2Ru(tpphen)Ru(bpy)\text{-}(OH_2)]^{4+}$, Cat/Substrate/$[Co^{III}(NH_3)_5Cl]^{2+}$ ratio = 1/500/1000; [c] Mn-TMPS (Mn(III)-5,10,15,20-tetrakis (2,4,6-trimethyl-3-sulfonatophenyl)porphyrin 0.1 mM, Cat/$[Ru^{III}(bpy)_3]^{2+}$/Substrate/$[Co^{III}(NH_3)_5Cl]^{2+}$ ratio = 1/10/1000/1000.

We thus thought about investigating other sulfide derivatives that could lead to an enantioselective sulfoxidation under the same conditions. In this respect, we were inspired by the epoxidation of

p-methoxy-styrene by oxone, in the presence of the Mn-TCPP-Xln10A hybrid as catalyst, which was previously demonstrated to be highly enantioselective (80% ee in favor of the *R* isomer). This was due to a preferential orientation of the *re* face of the styrene derivative towards the manganese-oxo oxidizing intermediate, provided by the formation of a H-bond between the O atom of the *p*-methoxy substituent and tyrosine 172 of Xln10A (Scheme 3A) [18]. We thus thought about using *p*-methoxy-thioanisole as substrate, expecting that in a similar way to *p*-methoxy-styrene, an H-bond between the O atom of the *p*-methoxy substituent and tyrosine 172 of Xln10A would preferentially orientate the sulfide towards the Mn-porphyrin-derived oxidizing species in order to get the R sulfoxide (Scheme 3B). The photoassisted sulfoxidation of 84 mM p-methoxy-thioanisole (2700 eq.) was then assayed in 50 mM phosphate buffer solution (pH 7.0) under the same conditions as those previously used for thioanisole.

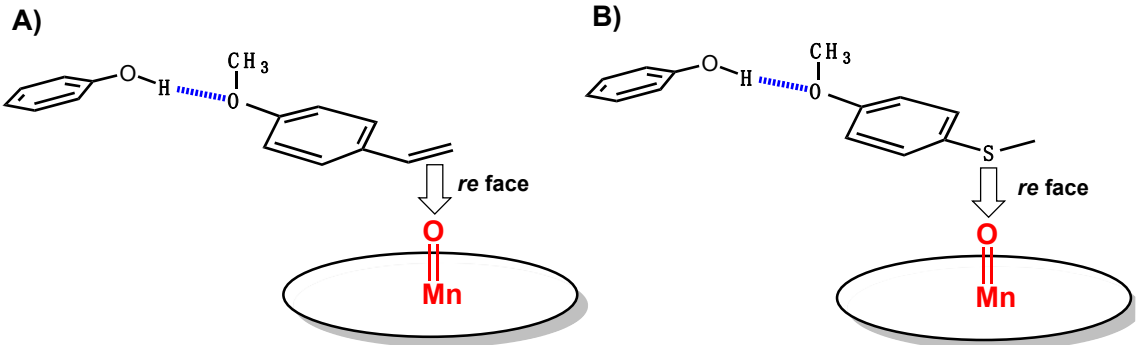

Scheme 3. Selective orientation of (**A**) *p*-methoxystyrene and (**B**) *p*-methoxythioanisole towards the putative porphyrin-Mn-oxo oxidizing species using **1**-Mn-Xln10A as catalyst

When **1**-Mn alone was used as an oxidizing catalyst, methyl-*p*-methoxyphenylsulfoxide was obtained as the only product with a TON of 100 ± 4 (51% yield with respect to $[Co^{III}(NH_3)_5Cl]^{2+}$), but the reaction was not stereoselective, as no enantiomeric excess could be measured after HPLC analysis. When the same reaction was performed in the presence of Xln10A, methyl-*p*-methoxyphenylsulfoxide was formed with a TON of 10 ± 1 (5% yield with respect to $[Co^{III}(NH_3)_5Cl]^{2+}$), but this time an enantiomeric excess of 7% ± 1% in favor of the R Isomer could be measured, showing that under those conditions the protein induced a slight stereoselectivity in favor of the expected *R*-isomer.

*2.3. Influence of the Xln10A/**1**-Mn Ratio on Catalysis*

The influence of the Xln10A/**1**-Mn ratio on the stereo selectivity was investigated. For this purpose, the oxidation of 116 mM methoxy-thioanisole in 50 mM phosphate buffer solution (pH 7.0) was performed in the presence of 0.42 mM $[Ru^{II}(bpy)_3]^{2+}$ (14 eq.) and 12 mM $[Co^{III}(NH_3)_5Cl]^{2+}$ (390 eq.), as described above, using 37.0 µM **1**-Mn (1 eq.) as catalyst in the presence of increasing amounts of xylanase 10A, ranging from 37.0 µM (1 eq.) to 148 µM (4.2 eq.). After extraction and analysis of the products, it appeared that the TON decreased from 54 to 24 TON when the Xln10A/**1**-Mn ratio increased from 1 to 4.2, whereas, surprisingly, no change in the enantiomeric excess was observed. One likely explanation for this could be that, when the protein is in excess with respect to **1**-Mn, it acts as a competitive substrate for the electron withdrawing reaction by the highly oxidative $[Ru^{II}(bpy)_3]^{3+}$ complex, leading to protein radicals that would initiate protein oligomerization. Further experiments were then performed to verify this hypothesis using sodium dodecyl sulfate polyacrylamide gel electrophoresis (SDS-PAGE) analysis of the protein.

2.4. Evolution of the Catalyst during the Reaction

To explain the weak enantiomeric excesses observed during the light-induced oxidation of thioanisole derivatives, the xylanase 10A protein was examined by denaturing SDS-PAGE after the reaction. This experiment was performed with 130 µM Xln10A as catalyst in 50 mM phosphate

buffer solution (pH 7.0), with 99 mM thioanisole, 0.42 mM $[Ru^{II}(bpy)_3]^{2+}$, 12 mM $[Co^{III}(NH_3)_5Cl]^{2+}$, and 32.5 μM **1**-Mn (Figure 2).

As shown in Figure 2, the starting pure Xln10A was characterized by a concentrated single band at 32 kDa, indicative of monomeric form, whereas, after the reaction, a band at higher MW (>250 kDa) could be observed, showing potential oligomerization of the protein over the course of the reaction.

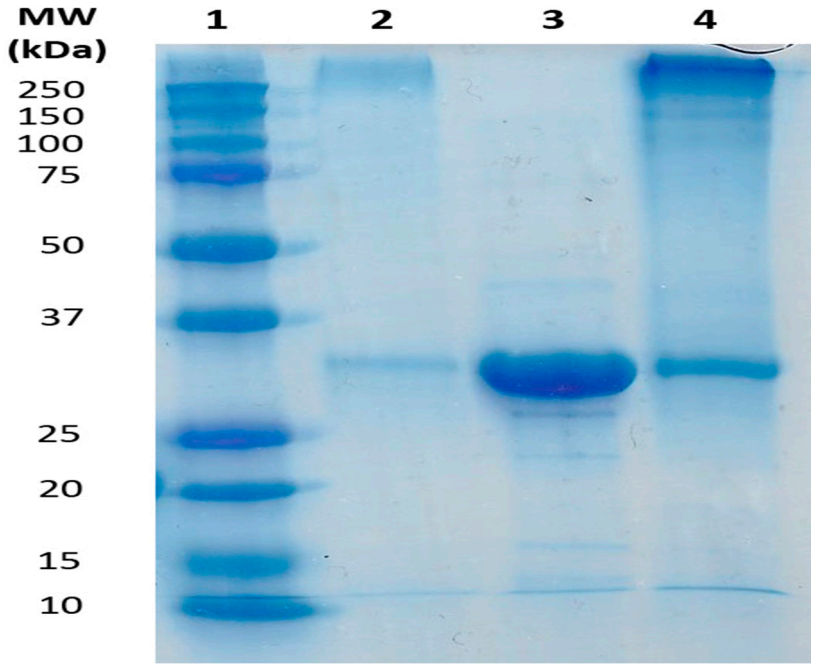

Figure 2. Sodium dodecyl sulfate polyacrylamide gel electrophoresis (SDS-PAGE) analysis of xylanase 10A. lane 1, molecular weight markers; lane 2, analysis of the pellet obtained after centrifugation of the reaction medium after the light induced oxidation reaction; lane 3, xylanase 10A purified before the reaction; lane 4, supernatant obtained after centrifugation of the reaction medium after catalysis.

2.5. Mechanistic Studies

Labeling experiments were realized to determine the origin of the oxygen atom of the obtained sulfoxide. Thus, the oxidation of *p*-methoxy-thioanisole was assayed under the same conditions as reported above, but 19.4% $H_2{}^{18}O$ was introduced for the preparation of the 50 mM phosphate buffer (pH 7.0) solvent. After extraction with ethyl acetate, the products were analyzed by High resolution (HR)-ESI MS. Twenty percent of the resulting sulfoxide contained ^{18}O, as shown by the peaks observed at 171.0480 and 173.0477 that correspond to $[M + H]^+$ species for $CH_3S^{16}OC_6H_5$ and $CH_3S^{18}OC_6H_5$ methyl phenyl sulfoxides, respectively (Figure 3). This confirmed that the inserted O-atom in the oxidation product originated from water molecules of the solvent medium.

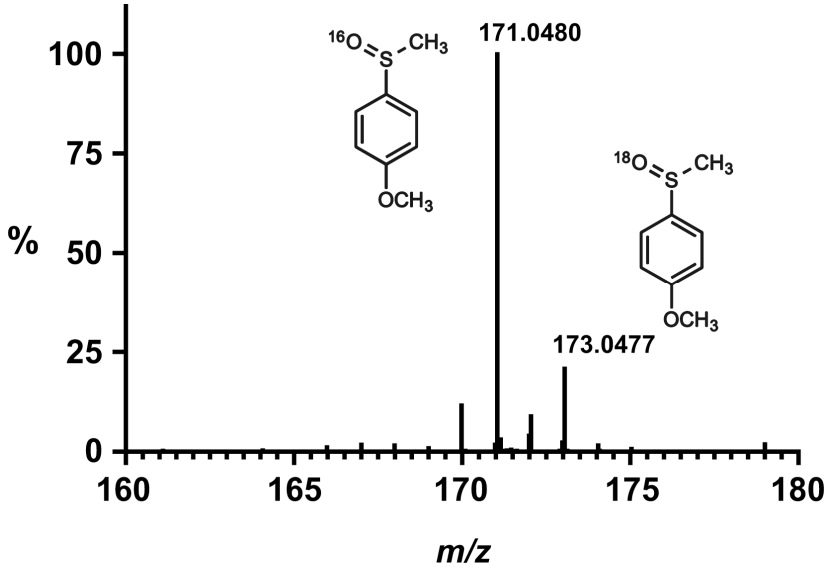

Figure 3. High-resolution Electron Spray Ionisation-Mass (ESI-MS) spectrum of the *p*-methoxy-thioanisole sulfoxide, obtained after the photoassisted oxidation of *p*-methoxy-thioanisole, in the presence of $[Ru^{II}(bpy)_3]^{2+}$, $[Co^{III}(NH_3)_5Cl]^{2+}$ and **1**-Mn-Xln10A as catalyst, in 50 mM phosphate buffer (pH 7.0) containing 19% $H_2{}^{18}O$. Peaks at 171.0480 and 173.0477 correspond to $[M + H]^+$ species for $CH_3SOC_6H_5$ and $CH_3S^{18}OC_6H_5$ methyl phenyl sulfoxide, respectively.

3. Discussion

The aforementioned results show that both the manganese(III)-meso-tetrakis-*para*-carboxyphenylporphyrin **1**-Mn and its complex with xylanase 10A, the **1**-Mn-Xln 10A hemozyme, catalyze the photo-assisted oxidation of thioanisole derivatives with formation of the sulfoxide as major product (Scheme 2, Table 1). With both thioanisole and *p*-methoxy-thioanisole, the reaction is highly chemoselective and leads to the corresponding sulfoxide as a major product with greater yields with **1**-Mn alone as catalyst (125 ± 5 TON and 100 ± 4 TON, respectively) than with **1**-Mn-Xln10A as catalyst (25 ± 2 TON and 10 ± 1 TON, respectively). This could indicate that the insertion of **1**-Mn into the hydrophobic pocket of Xln10A [18] hinders the electron transfer from the manganese center to the photo-activated ruthenium complex. The results observed in the presence of **1**-Mn-Xln10A are, however, comparable to those obtained under the same conditions for the oxidation of thioanisole catalyzed by an Mn-corrole complex and Mn-corrole-BSA artificial metalloenzyme, which respectively lead to the chemoselective formation of the corresponding sulfoxide with 32 ± 3 and 21 ± 7 TON (Table 1) [17]. In addition, as studies in the presence of $H_2{}^{18}O$ show the incorporation of ^{18}O in the obtained sulfoxide, and no reaction occurs in the absence of the $[Ru^{II}(bpy)_3]^{2+}$ photoactivator, it is reasonable to propose that the reaction follows a mechanism similar to that depicted in Scheme 1. Water would thus act as the oxygen source, leading to an Mn^{III}-OH that would be oxidized into an Mn^{IV}-oxo species by the photogenerated highly oxidative $[Ru^{III}(bpy)_3]^{3+}$ species. For the **1**-Mn homogenous catalyst, the final Mn^{V}-oxo oxidizing species would likely arise from the disproportionation of the Mn^{IV}-oxo species into Mn^{III} and Mn^{V}=O (Scheme 1, Path b) as reported for other manganese porphyrin complexes [15,16] whereas it would be formed upon oxidation of the Mn^{IV}-oxo by the photogenerated $[Ru^{III}(bpy)_3]^{3+}$ in the **1**-Mn-Xln10A system (Scheme 1, pathway a) [14] because disproportionation between complexes embedded in Xln10A is unlikely.

Since the oxidation of 2-(CH_3-thio)ethanol catalyzed by the Mn(III)-5,10,15,20-tetrakis (2,4,6-trimethyl-3-sulfonatophenyl)porphyrin (Mn-TMPS) under the same conditions was also reported to lead to the formation of the corresponding sulfoxide with 30 TON (Table 1) [16], **1**-Mn-Xln10A is an equally interesting artificial metalloenzyme for the chemoselective photoinduced oxidation of sulfides in water. It is noteworthy, however, that these results illustrate lower yields relative to

those obtained in the presence of supramolecular assemblies in which a ruthenium-tris-bipyridyl photoactivable moiety (Ru_{Phot}) is covalently attached to another Ru(tpy)(bpy)(H_2O) catalytic moiety (Ru_{cat}) that photoinduces the sulfoxidation of thioanisole derivatives, such as thioanisole, *p*-Methoxy-, and *p*-bromo-thioanisole using water as an oxygen source, in the presence of $[Co^{III}(NH_3)_5Cl]^{2+}$ as sacrificial reductant with 200–745 TON (Table 1) [22,23].

As expected, no enantioselectivity was observed for the oxidation of thioanisole and *p*-methoxy thioanisole with that of **1**-Mn alone as catalyst (Table 1). Surprisingly, no enantioselectivity could be observed for the oxidation of thioanisole in the presence of Xln10A, which contrasted with the 12%–16% ee observed for the same reaction in the presence of Mn-Corrole-BSA as catalyst [17] (Table 1). The oxidation of *p*-methoxy-thioanisole, which was chosen in the hope of a selective pro-R positioning of the sulfide similar to that previously reported for *p*-methoxy-styrene [18] (Scheme 3) was only slightly enantioselective, though it led to the R sulfoxide as the major enantiomer, as was expected. However, the ee value, 7% ± 1%, was far from that obtained for the epoxidation of *p*-methoxy-styrene by oxone catalyzed by **1**-Mn-Xln10A, (80% ee in favor of the R epoxide). This could be due to a denaturation of the protein during catalysis. Indeed, when the Xln10A/**1**-Mn ratio increases, the ee remains constant, whereas the TON decreases, in agreement with a radical polymerization initiated by its direct reaction with the $[Ru^{II}(bpy)_3]^{3+}$ intermediate.

4. Materials and Methods

4.1. Physical Measurements

ESI-HRMS was determined on a micrOTOF-Q II 10027 apparatus (Bruker Daltonics, Billerica, MA, USA), UV/Vis spectra were recorded on an UVIKON-XL spectrophotometer (BioTek Instruments, Inc., Winooski, VE, USA) fluorescence spectra were recorded on a CARY Eclipse fluorometer (Agilent Technologies, Santa Clara, CA, USA). Gas chromatographs (Shimadzu Scientific Instruments, Inc., Columbia, MA, USA) were obtained with a Shimazu GC 2010 plus apparatus equipped with a Zebron ZB-SemiVolatiles Gas Chromatography (GC) column (30 m × 0.25 mm × 0.25 µm). HPLC (Agilent Technologies, Santa Clara, CA, USA) was performed on an Agilent Infinity 1260 apparatus equipped with a chiral column (Chiralcel OD-H, Daicel Co., Osaka, Japan, 250 mm × Φ4.6 mm).

*4.2. Synthesis of Mn^{III}-meso-tetrakis(para-carboxyphenyl)porphyrin (**1**-Mn)*

meso-Tetrakis(*para*-carboxyphenyl)porphyrin (**1**) was prepared in 10.5% yield by condensation of p-carboxybenzaldehyde with pyrrole in propionic acid according to the procedure of Adler et al. [19,20], and its molecular properties were found to be identical to those already reported [19]: ^{1}H-NMR (d_6-DMSO) 8.85 (8H, s), 8.38 (8H, d, J = 8 Hz), 8.32 (8H, d, J = 8 Hz), −2.95 (2H, s, NH); Matrix-assisted Laser Desorption-Time Of Flight (MALDI-TOF)-MS: m/z = 791.21 (M + H^+). The insertion of manganese was performed by treatment of **1** (2.5 mM) in AcONa buffer (pH 4.0, 50 mM) with $Mn(OAc)_2$, $4H_2O$ (11 equiv.) at 100 °C for 4 h. The progress of the reaction was monitored by UV/Vis spectroscopy. After 2 h under reflux, the Mn metalation was quantitative. The excess of manganese salt was then removed by successive purifications on P6DG exclusion gel and then on Chelex. After lyophylisation, **1**-Mn was obtained as a purple solid in a quantitative yield. Its properties were found to be identical to those already reported [18]: UV/Vis (pH 7.0, sodium phosphate buffer, 50 mM): λ_{max} (ε): 468 (93×10^3 $M^{-1}\cdot cm^{-1}$), 565, 600 nm; MALDI HR-MS (ESI): m/z = 843.12396, calculated for $C_{48}H_{28}MnN_4O_8$, and m/z = 843.12132 (Δm = 5.04 ppm).

*4.3. Preparation and Characterization of the Artificial Metalloenzyme **1**-Mn-Xln10A*

Xylanase 10A was first purified from the supernatant of *S. lividans* culture as reported earlier [19]. The various **1**-Mn-Xln10A hemozyme samples were then prepared by incubation for 30 min at room temperature (RT) of Xln10A in sodium phosphate buffer (50 mM, pH 7.0) with various amounts of

1-Mn. **1**-Mn-Xln10A was then characterized by UV/Vis and fluorescence spectroscopy studies as already reported [18].

4.4. UV/Vis Spectroscopy Experiments

1-Mn (5 μM) was incubated with Xln10A (1.5 equiv.) in 50 mM sodium phosphate buffer (pH 7.0) at room temperature for 30 min, and the UV/Vis spectrum was recorded between 280 nm and 700 nm. The spectrum obtained was found identical to that already reported [18]: UV/Vis (pH 7.0, sodium phosphate buffer, 50 mM): λ_{max} (ε): 468 (92.3×10^3 $M^{-1} \cdot cm^{-1}$), 565,600 nm.

4.5. Determination of the K_D Values for **1***-Mn-Xln10A Complexes*

The K_D value for **1**-Mn-Xln10A complexes as well as the **1**-Mn/Xln10A stoichiometry were determined as follows: the fluorescence spectrum of Xln10A, 5 μM in 50 mM sodium phosphate buffer, pH 7.2, at 25 °C was first recorded between 300 and 400 nm after excitation of the sample at 290 nm. The quenching of fluorescence was then followed by progressive addition of a 500 μM solution of **1**-Mn in 50 mM phosphate buffer pH 7.0. A double reciprocal plot of the residual fluorescence intensity at 340 nm as a function of the **1**-Mn final concentration afforded a K_D value of 1.5 μM for the **1**-Mn-Xln10A complex and a 1/1 **1**-Mn/Xln10A stoichiometry.

4.6. Photoassisted Oxidation of Sulfides

For a typical photo-oxidation reaction, 150 μM of pure xylanase 10A, 37.5 μM porphyrin, 130 μL of 3.04 mM $[Ru^{II}(bpy)_3]^{2+}$ in phosphate buffer saline PBS, and either 11 μL thioanisole or 30 μL 4-methoxy thioanisole were added to a 800 μL degassed 50 mM phosphate buffer solution (pH 7.0) containing 14 mM $[Co^{III}(NH_3)_5Cl]^{2+}$. The solution was degassed by three freeze/thaw cycles, and the samples were illuminated with a 450 nm diode and stirred for 10 minutes at RT. The final concentrations of each component were 12 mM $[Co^{III}(NH_3)_5Cl]^{2+}$ (390 eq.), 130 μM xylanase 10A (4.2 eq.), 32.5 μM Mn-porphyrin (1 eq.), 0.42 mM $[Ru^{II}(bpy)_3]^{2+}$ (14 eq.), and 84 mM 4-methoxy thioanisole (2700 eq.), or 99 mM thioanisole (3200 eq.). Control experiments without protein were performed maintaining the above concentrations. Control experiments without chromophore were performed by substituting the $[Ru^{II}(bpy)_3]^{2+}$ solution by the equivalent PBS solution.

4.7. Extraction and Analysis of the Oxidation Products

After reaction, the content of the vial was eluted through a short (3 cm) silica plug to which 100 μL 10^{-2} M acetophenone solution acting as internal standard had been previously added. The column was washed with 2 mL ethyl acetate in order to elute all the components. The aqueous phase of the resulting filtrate was removed and the organic phase was dried using $NaSO_4$ prior to GC analysis. For detection of thioanisole and its oxidation products, the applied temperature gradient was as follows: from 100 °C to 130 °C at 5 °C/min, and then 130 °C to 300 °C at 50 °C/min, which was further held constant for 3 min. The injector and flame injector detection (FID) temperature were set at 300 °C. Elution retention times were (min): acetophenone (4.03), thioanisole (4.32), thioanisole sulfoxide (7.56), and thioanisole sulfone (8.04). To study the enantiomeric excess of the obtained sulfoxide, the solvent was evaporated and the residue was re-dissolved in the minimum amount of isopropanol prior to HPLC analysis. The enantiomeric excesses were then determined by HPLC analysis using a chiral column (Chiralcel OD-H, Daicel Co., IlKirch, France, 250 mm × Φ4.6 mm). For the oxidation of thioanisole, samples were eluted with hexane/isopropanol (95:5, *v*/*v*, 1.0 mL/min), and, for the oxidation of *p*-methoxy-thioanisole, elution was done with hexane/isopropanol (97:3, *v*/*v*, 1.2 mL/min). All products were detected at 254 nm. Authentic samples of each sulfoxide enantiomer were prepared by the method previously described by Li et al. [24], and their retention time under the above described conditions are, respectively, 17 min and 21 min. for the *R* and *S* thioanisole sulfoxides, and 32 min and 36 min. for the *R* and *S* *p*-methoxy-thioanisole sulfoxides.

5. Conclusions

The aforementioned results demonstrate that an anionic manganese porphyrin, Mn(III)-meso-tetrakis-*para*-carboxyphenylporphyrin **1**-Mn, as well as its complex with xylanase 10A, the **1**-Mn-Xln10A artificial metalloenzyme, can be activated by visible light via a ruthenium chromophore. The resulting oxidized form of these complexes was found to catalyze the chemoselective and slightly enantioselective oxidation of thioanisole derivatives into the corresponding sulfoxides. The presence of $H_2{}^{18}O$ in the reaction medium led to the insertion of ^{18}O in the product, which confirmed the role of water as the O-atom source in the reaction. Thus, our results clearly illustrate that oxidation catalysis can be performed in aqueous medium, using no other oxygen atom source than water itself and using visible light as the only energy input. A slight enantiomeric excess in favor of the *R* sulfoxide could be obtained, which is likely to be related to protein polymerization and could be initiated by its direct reaction with intermediate ruthenium or Mn-porphyrin active species outside the binding site. A better strategy to limit those reactions, and then to increase the stereoselectivity of the reaction, could consist of covalently attaching the Ru complex to the protein, in a place close the catalyst, in order to minimize oxidation of the protein backbone, as it has already been realized in the case of cytochromes P450 [12,13].

Acknowledgments: This work was partly supported by the Programme Samuel-De-Champlain from the Commission Permanente de Coopération Franco-Québécoise (CPCFQ), by the LabEx de Chimie des Architectures Moléculaires Multifonctionnelles et des Matériaux (CHARM$_3$AT), by the ANR (project ANR Blanc Cathymetoxy (ANR-11-BS07-024) and by a Natural Sciences and Engineering Research Council of Canada (NSERC) Discovery Grant RGPIN 2016-05557 (to N.D.). D.G. held an NSERC Alexander Graham Bell Canada Graduate Scholarship.

Author Contributions: Christian Herrero and Rémy Ricoux conceived and designed the experiments; Donald Gagné, Fabien Hammerer, and Nhung Nguyen-Thi performed the experiments and contributed reagents/materials/analysis tools, Christian Herrero and Rémy Ricoux analyzed the data; Jean-Pierre Mahy, Frédéric Banse, Rémy Ricoux, and Nicolas Doucet wrote the paper.

Conflicts of Interest: The authors declare no conflict of interest.

References

1. Li, C.J.; Anastas, P.T. Green Chemistry: present and future. *Chem. Soc. Rev.* **2012**, *41*, 1413–1414. [CrossRef] [PubMed]
2. Conley, B.L.; Tenn, W.J.; Young, K.J.H.; Ganesh, S.K.; Meier, S.K.; Ziatdinov, V.R.; Mironov, O.; Oxgaard, J.; Gonzales, J.; Goddard, W.A.; et al. Desig and study of homogeneous catalysts for the selective, low temperature oxidation of hydrocarbons. *J. Mol. Catal. A* **2006**, *251*, 8–23. [CrossRef]
3. Labinger, J.A. Selective alkane oxidation: Hot and cold approaches to a hot problem. *J. Mol. Catal. A* **2004**, *220*, 27–35. [CrossRef]
4. Collins, T.J. TAML oxidant activators: A new approach to the activation of hydrogen peroxide for environmentally significant problems. *Acc. Chem. Res.* **2002**, *35*, 782–790. [CrossRef] [PubMed]
5. Andersen, O.A.; Flatmark, T.; Hough, E. Crystal structure of the ternary complex of the catalytic domain of human phenylalanine hydroxylase with tetrahydrobiopterin and 3-(2-thienyl)-L-alanine and its implications for the mechanism of catalysis and substrate activation. *J. Mol. Biol.* **2002**, *320*, 1095–1108. [CrossRef]
6. Tinberg, C.E.; Lippard, S.J. Dioxygen Activation in Soluble Methane Monooxygenase. *Acc. Chem. Res.* **2011**, *44*, 280–288. [CrossRef] [PubMed]
7. Sirajuddin, S.; Rosenzweig, A.C. Enzymatic oxidation of methane. *Biochemistry* **2015**, *54*, 2283–2294. [CrossRef] [PubMed]
8. Hrycay, E.G.; Bandiera, S.M. Monooxygenase, peroxidase and peroxygenase properties and reaction mechanisms of cytochrome P450 enzymes. *Adv. Exp. Med. Biol.* **2015**, *851*, 1–61. [PubMed]
9. Iyanagi, T.; Xia, C.; Kim, J.J. NADPH-cytochrome P450 oxidoreductase: Prototypic member of the diflavin reductase family. *Arch. Biochem. Biophys.* **2012**, *528*, 72–89. [CrossRef] [PubMed]
10. Meunier, B.; Robert, A.; Pratviel, G.; Bernadou, J. Metalloporphyrins in catalytic oxidations and oxidative DNA cleavage. In *The Porphyrin Handbook*; Kadish, K.M., Smith, K., Guilard, R., Eds.; Academic Press: San Diego, FL, USA, 2000; Volume 4, pp. 119–184.

11. Meunier, B. Metalloporphyrins as versatile catalysts for oxidation reactions and oxidative DNA cleavage. *Chem. Rev.* **1992**, *92*, 1411–1456. [CrossRef]
12. Tran, N.H.; Nguyen, D.; Dwaraknath, S.; Mahadevan, S.; Chavez, G.; Nguyen, A.; Dao, T.; Mullen, S.; Nguyen, T.A.; Cheruzel, L.E. An Efficient Light-Driven P450 BM3 Biocatalyst. *J. Am. Chem. Soc.* **2013**, *135*, 14484–14487. [CrossRef] [PubMed]
13. Ener, M.E.; Leeb, Y.-T.; Winkler, J.R.; Gray, H.B.; Cheruzel, L.E. Photooxidation of cytochrome P450-BM3. *Proc. Natl. Acad. Sci. USA* **2010**, *107*, 18783–18786. [CrossRef] [PubMed]
14. Kato, M.; Nguyen, D.; Gonzalez, M.; Cortez, A.; Mullen, S.E.; Cheruzel, L.E. Regio- and stereoselective hydroxylation of 10-undecenoic acid with a light-driven P450 BM3 biocatalyst yielding a valuable synthon for natural product synthesis. *Bioorg. Med. Chem.* **2014**, *22*, 5687–5691. [CrossRef] [PubMed]
15. Maliyackel, A.C.; Otvos, J.W.; Spreer, L.O.; Calvin, M. Photoinduced oxidation of a water-soluble manganese(III) porphyrin. *Proc. Natl. Acad. Sci. USA* **1986**, *83*, 3572–3574. [CrossRef] [PubMed]
16. Fukuzumi, S.; Kishi, T.; Kotani, H.; Lee, Y.-M.; Nam, W. Highly efficient photocatalytic oxygenation reactions using water as an oxygen source. *Nat. Chem.* **2011**, *3*, 38–41. [CrossRef] [PubMed]
17. Herrero, C.; Quaranta, A.; Ricoux, R.; Trehoux, A.; Mahammed, A.; Gross, Z.; Banse, F.; Mahy, J.P. Oxidation catalysis via visible-light water activation of a $[Ru(bpy)_3]^{2+}$ chromophore BSA–metallocorrole couple. *Dalton Trans.* **2016**, *45*, 706–710. [CrossRef] [PubMed]
18. Allard, M.; Dupont, C.; Munoz Robles, V.; Doucet, N.; Lledos, A.; Marechal, J.-D.; Urvoas, A.; Mahy, J.-P.; Ricoux, R. Incorporation of manganese complexes into xylanase: New artificial metalloenzymes for enantioselective epoxidation. *ChemBioChem* **2012**, *13*, 240–251. [CrossRef] [PubMed]
19. Ricoux, R.; Allard, M.; Dubuc, R.; Dupont, C.; Marechal, J.-D.; Mahy, J.-P. Selective oxidation of aromatic sulfide catalyzed by an artificial metalloenzyme: New activity of hemozymes. *Org. Biomol. Chem.* **2009**, *7*, 3208–3211. [CrossRef] [PubMed]
20. Adler, A.D.; Longo, F.R.; Finarelli, J.D.; Goldmacher, J.; Assour, J.; Korsakoff, L.J. A simplified synthesis for meso-tetraphenylporphine. *J. Org. Chem.* **1967**, *32*, 476. [CrossRef]
21. Ricoux, R.; Dubuc, R.; Dupont, C.; Marechal, J.D.; Martin, A.; Sellier, M.; Mahy, J.P. Hemozymes peroxidase activity of artificial hemoproteins constructed from the *Streptomyces lividans* xylanase a and Iron(III)-carboxy-substituted porphyrins. *Bioconj. Chem.* **2008**, *19*, 899–910. [CrossRef] [PubMed]
22. Li, T.-T.; Li, F.-M.; Zhao, W.-L.; Tian, Y.-H.; Chen, Y.; Cai, R.; Fu, W.-F. Highly efficient and selective photocatalytic oxidation of sulfide by a chromophore-catalyst dyad of ruthenium-based complexes. *Inorg. Chem.* **2015**, *54*, 183–191. [CrossRef] [PubMed]
23. Hamelin, O.; Guillo, P.; Loiseau, F.; Boissonnet, M.-F.; Menage, S. A Dyad as photocatalyst for light-driven sulfide oxygenation with water as the unique oxygen atom source. *Inorg. Chem.* **2011**, *50*, 7952–7954. [CrossRef] [PubMed]
24. Li, A.T.; Zhang, J.D.; Xu, J.H.; Lu, W.Y.; Lin, G.Q. Isolation of *Rhodococcus* sp. ECU0066, a new sulfide monooxygenase producing strain for asymmetric sulfoxidation. *Appl. Environ. Microbiol.* **2009**, *75*, 551–556. [CrossRef] [PubMed]